PHYSICAL REVIEW A VOLUME 39, NUMBER 6 MARCH 15, 1989

Theory of transitions among tilted hexatic phases in liquid crystals

Jonathan V. Selinger and David R. Nelson
Department of Physics, Harvard University, Cambridge, Massachusetts 02138
(Received 26 October 1988)

We present a Landau theory for transitions among tilted hexatic phases in liquid-crystal films. Using the renormalization group, we then derive phase diagrams with four tilted hexatic phases: the hexatic-I and hexatic-F phases, an intermediate hexatic-L phase, and an unlocked phase. If the films are crystalline rather than hexatic, all these phases except the unlocked phase still exist. These results are consistent with recent experiments on thermotropic and lyotropic liquid crystals. We also study the five-armed "star" defect close to the hexatic-to-hexatic transitions. Near the first-order transition from hexatic-I to hexatic-F, the thickness of the arms increases as $|T-T_{IF}|^{-1/3}$ through a process similar to wetting. This thickening should be observable in thin tilted hexatic films.

I. INTRODUCTION

Layered liquid-crystal systems have a rich variety of phases with different types of in-plane two-dimensional (2D) order. Among the most interesting are the tilted hexatic phases. These phases have at least quasi-long-range order in two order parameters: the orientation of the six local in-plane bonds and the direction of the local molecular tilt. They have only short-range in-plane crystalline order. Tilted hexatic phases can differ from each other in the relation between the local tilt and bond directions. In the hexatic-I phase, the local tilt (azimuthal) angle is locked along one of the local bonds. In the hexatic-F phase, the local tilt angle is locked halfway between two local bonds, 30° from each. In the hexatic-L phase, the local tilt is locked at an angle between 0° and 30° from a local bond.[1] There may also be an unlocked phase, in which the bond and tilt angles fluctuate independently.[2]

Recent experiments have investigated transitions among tilted hexatic phases in two different systems. First, Dierker and Pindak[3] have studied tilted hexatic phases in five-layer films of thermotropic liquid crystals. They observe a direct phase transition from hexatic-I to -F. This transition is weakly first order, with large pretransitional anomalies. Second, Smith *et al.*[1] have examined the $L_{\beta'}$ phases of lyotropic liquid crystals. These phases are probably hexatic because of dislocation buckling (see Sec. V), but they may contain finite in-plane crystallites. Smith *et al.* find three $L_{\beta'}$ phases: the $L_{\beta I}$ and $L_{\beta F}$ phases and a new intermediate $L_{\beta L}$ phase, which are the lyotropic analogues of the hexatic-I, -F, and -L phases. The $L_{\beta I}$-$L_{\beta L}$ and $L_{\beta L}$-$L_{\beta F}$ transitions are second order.

In an earlier paper,[4] we developed a Landau theory with fluctuation corrections for transitions among tilted hexatic phases. In this paper we discuss that theory in greater detail, and we use it to investigate finite-size effects. We also predict the behavior of the Dierker-Pindak-Meyer "star" defect[5] near the hexatic-to-hexatic transitions. These predictions could be tested by experiments on thin tilted hexatic films.

The basic physics behind our model can be seen in a simple mean-field theory. Let $\theta(\mathbf{r})$ be the bond-angle field and $\phi(\mathbf{r})$ be the tilt-azimuthal-angle field. As a first approximation, we neglect fluctuations in these fields. In this paper we use the tilt-bond interaction potential

$$V(\theta-\phi)=-h_6\cos[6(\theta-\phi)]-h_{12}\cos[12(\theta-\phi)]\ . \tag{1.1}$$

Suppose that h_{12} is fixed at a *negative* value, and h_6 decreases from positive to negative values as we adjust some external field, such as temperature or humidity. The sequence of potentials is shown in Fig. 1. For $h_6>4|h_{12}|$ the only minimum is at $\theta_-\equiv\theta-\phi=0°$ (mod 60°). The system is in the I phase, with the tilt locked along one of the local bonds. As h_6 passes through $4|h_{12}|$, the minimum at $\theta_-=0°$ becomes quartic and then splits into two equally deep minima at $\theta_-=\pm\frac{1}{6}\cos^{-1}(h_6/4|h_{12}|)$. We therefore have an Ising-type, second-order, symmetry-breaking transition from I to L at $h_6=4|h_{12}|$. As h_6 decreases from $+4|h_{12}|$ to $-4|h_{12}|$, the minima in the L phase shift smoothly from $\theta_-=0°$ to $\pm30°$. At $h_6=-4|h_{12}|$ there is another Ising-type, second-order transition from L to F, and F remains the stable phase for all $h_6<-4|h_{12}|$. This behavior is essentially what Smith *et al.*[1] observe by varying humidity in the $L_{\beta'}$ phases. By contrast, if h_{12} is *positive*, then the potential passes through the sequence shown in Fig. 2, and the system has a direct, first-order transition from I to F at $h_6=0$. This behavior is essentially what Dierker and Pindak[3] observe by varying temperature in thermotropic films.

The plan of this paper is as follows. In Sec. II we construct a general Hamiltonian for the fluctuating fields $\theta(\mathbf{r})$ and $\phi(\mathbf{r})$, and we define a complex order parameter that describes all of the hexatic-to-hexatic transitions. In Sec. III we discuss the mean-field theory introduced above in more detail. In Sec. IV we use the renormalization group to analyze the effects of fluctuations in $\theta(\mathbf{r})$ and $\phi(\mathbf{r})$ in two dimensions. Fluctuations change qualitatively the mean-field results sketched above at sufficiently high temperatures or low elasticities. We derive phase di-

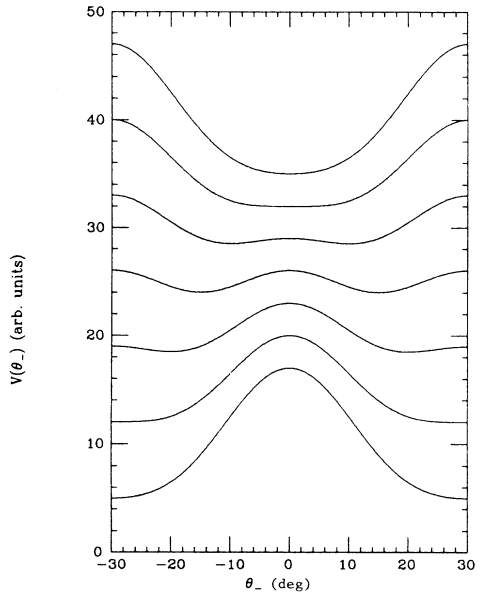

FIG. 1. Sequence of potentials (1.1) with $h_{12}=-1$ and $h_6=6$, 4, 2, 0, -2 -4, and -6 (top to bottom). In mean-field theory, there are Ising-type second-order transitions at $h_6=\pm 4|h_{12}|$.

agrams showing the I, L, and F phases as well as the unlocked phase, and we make several universal predictions. We also discuss how our results are modified by finite-size effects. In Sec. V we compare our phase diagrams with experiments. In addition, we show that all the phases except the unlocked phase exist if there is 2D crystalline order as well as bond-orientational order. Our theory therefore applies to the $L_{\beta'}$ phases whether they are hexatic or crystalline.

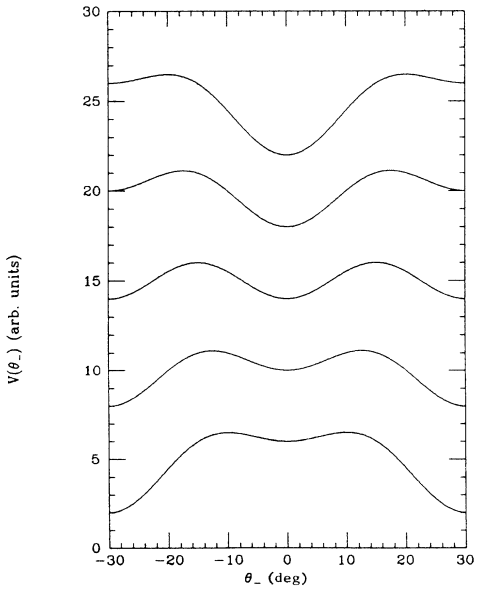

FIG. 2. Sequence of potentials (1.1) with $h_{12}=1$ and $h_6=2$, 1, 0, -1, and -2 (top to bottom). There is a first-order transition at $h_6=0$.

In Sec. VI we examine the five-armed star defect of tilted hexatic phases. Dierker, Pindak, and Meyer[3,5] have observed this defect in thin films of thermotropic liquid crystals, which have a direct, first-order I-F transition. According to our theory, the arms thicken near the first-order transition, and each arm contains a sliver of the incipient, metastable phase. Through a mechanism analogous to wetting, the thickness of the arms increases as $|h_6|^{-1/3}$ or, equivalently, as $|T-T_{IF}|^{-1/3}$. This divergence is cut off when the arm thickness grows to a size proportional to the square root of the arm length. This thickening should be observable in thin tilted hexatic films. It may also be possible to observe the star defect in materials that have an L phase. According to our theory, inside the L phase the five arms become five wide petals. Each petal contains the mirror image of the bulk L phase.

II. HAMILTONIAN AND ORDER PARAMETER

In our theory we extend the work of Nelson and Halperin[2] by using a more general tilt-bond interaction. We consider the Hamiltonian for a 2D tilted hexatic membrane,

$$\frac{H}{k_BT}=\int d^2\mathbf{r}[\tfrac{1}{2}K_6|\nabla\theta|^2+\tfrac{1}{2}K_1|\nabla\phi|^2 +g\nabla\theta\cdot\nabla\phi+V(\theta-\phi)]\ . \tag{2.1}$$

The coefficient K_6 is a Frank constant for variations in the bond orientation $\theta(\mathbf{r})$, K_1 is a stiffness constant for variations in the tilt angle $\phi(\mathbf{r})$, and g is a gradient cross coupling. In this Hamiltonian we neglect elastic anisotropy, which we will discuss in Sec. V. The function $V(\theta-\phi)$ is a general tilt-bond interaction potential. Because of the local hexagonal symmetry, it can be expressed in general as the Fourier series

$$V(\theta-\phi)=-\sum_{n=1}^{\infty}h_{6n}\cos[6n(\theta-\phi)]\ . \tag{2.2}$$

If the potential is smooth, then $|h_{6n}|$ decreases rapidly with increasing n. Furthermore, we will show that h_{6n} becomes less relevant in the renormalization-group sense as n increases. For these reasons, inside the I and F phases the h_6 term is the dominant term, and one can neglect all the other terms, as in Ref. 2. However, our aim is to find the behavior near the transition from I to F, when h_6 passes through 0. Hence, we must also keep the h_{12} term, and we obtain the potential (1.1).

In this paper we consider only low-temperature phases, in which disclinations in $\theta(\mathbf{r})$ and vortices in $\phi(\mathbf{r})$ are rare. In the absence of these defects, we can treat both fields as single valued. We can then simplify the Hamiltonian (2.1) by defining the linear combinations[2]

$$\theta_+(\mathbf{r})=\alpha\theta(\mathbf{r})+\beta\phi(\mathbf{r})\ , \tag{2.3a}$$

$$\theta_-(\mathbf{r})=\theta(\mathbf{r})-\phi(\mathbf{r})\ , \tag{2.3b}$$

where $\alpha=1-\beta=(K_6+g)/(K_6+K_1+2g)$. In terms of $\theta_\pm(\mathbf{r})$, the Hamiltonian becomes

$$\frac{H}{k_B T} = \int d^2\mathbf{r}[\tfrac{1}{2}K_+|\nabla\theta_+|^2+\tfrac{1}{2}K_-|\nabla\theta_-|^2+V(\theta_-)] , \tag{2.4}$$

with $K_+ = K_6 + K_1 + 2g$ and $K_- = (K_1K_6 - g^2)/K_+$. The average value of θ_- is 0° (mod 60°) in the I phase, 30° (mod 60°) in the F phase, and between 0° and ±30° (mod 60°) in the L phase. Variations in $\theta_+(\mathbf{r})$ and $\theta_-(\mathbf{r})$ correspond to "acoustic" and "optical" modes, respectively, with in-phase and out-of-phase variations of bond and tilt angles.[3]

To describe all the tilted hexatic phases, we use the order parameter $M_- \equiv \langle e^{6i\theta_-} \rangle$. This order parameter is 0 in the unlocked phase (where its correlations decay algebraically[2]), real and positive in the I phase, real and negative in the F phase, and complex in the L phase. There are three ways for M_- to go from the positive real axis to the negative real axis: it can go continuously through 0, it can make a direct, finite jump from positive to negative, and it can go through the complex plane. In Secs. III and IV, we will show that all three of these possibilities occur in the phase diagram.

Before going on, we should make one more comment about the Hamiltonian (2.1). In writing this Hamiltonian, we implicitly assume that the membrane is flat. If the membrane is curved, then in the Hamiltonian we must replace $\nabla\theta$ by $\nabla\theta + \mathbf{A}$ and $\nabla\phi$ by $\nabla\phi + \mathbf{A}$, where $\mathbf{A}$ is a "vector potential" determined by the membrane curvature.[6-8] However, when we change variables from $\theta(\mathbf{r})$ and $\phi(\mathbf{r})$ to $\theta_+(\mathbf{r})$ and $\theta_-(\mathbf{r})$, the vector potential only affects the $\nabla\theta_+$ term.[9] Physically, because $\theta(\mathbf{r})$ and $\phi(\mathbf{r})$ can be measured relative to the same locally defined axis, the *difference* $\theta(\mathbf{r}) - \phi(\mathbf{r})$ does not experience any frustration due to membrane curvature. For this reason, membrane curvature does not affect the order parameter M_- or the phase diagram discussed in this paper.

III. MEAN-FIELD THEORY

As a first approximation, we neglect fluctuations in $\theta(\mathbf{r})$ and $\phi(\mathbf{r})$ and simply minimize the potential (1.1). In this mean-field theory, we determine how the minimum shifts as h_6 changes sign for fixed nonzero h_{12}.

In Sec. I we have already described the behavior for fixed *negative* h_{12}. As h_6 changes sign, the potential passes through the sequence shown in Fig. 1. At $h_6^{IL} = 4|h_{12}|$ there is a second-order, symmetry-breaking transition from the I phase, which has reflection symmetry, to the L phase, which lacks it. This transition is analogous to the Ising transition from the paramagnetic to the ferromagnetic phase, with h_6 analogous to temperature and $\mathrm{Im}M_-$ to magnetization. Just below h_6^{IL},

$$\mathrm{Im}M_- \propto \pm(h_6^{IL} - h_6)^{\beta} , \tag{3.1}$$

with $\beta = \frac{1}{2}$, as in mean-field theory for the Ising model. As h_6 decreases from h_6^{IL} to $h_6^{LF} = -4|h_{12}|$, the complex order parameter M_- passes through the complex plane from the positive real axis to the negative real axis. Just above h_6^{LF},

$$\mathrm{Im}M_- \propto \pm(h_6 - h_6^{LF})^{\beta} , \tag{3.2}$$

with $\beta = \frac{1}{2}$ as before. At h_6^{LF} reflection symmetry is restored by a second-order transition from L to F.

If h_{12} is fixed at a *positive* value, the behavior is quite different. As h_6 passes through 0, the potential goes through the sequence shown in Fig. 2. There can be local minima at $\theta_- = 0°$ and 30° (mod 60°). For $h_6 > 0$ the minimum at 0° is deeper, and the system is in the I phase. For $h_6 < 0$ the minimum at 30° is deeper, and the system is in the F phase. At $h_6 = 0$ there is a direct first-order transition from the I phase to the F phase. The order parameter M_- jumps discontinuously from the positive real axis to the negative real axis. We therefore obtain the phase diagram of Fig. 3.

Our mean-field theory of hexatic-to-hexatic transitions is analogous to the mean-field theory of surface tilt-angle transitions in nematic liquid crystals.[10] The surface texture of a nematic liquid crystal may be homeotropic (director normal to the surface), conical (director between 0° and 90° from the surface), or planar (director parallel to the surface). As the temperature changes, the surface texture may have a direct first-order transition from homeotropic to planar, or it may have a second-order transition from homeotropic to conical followed by another second-order transition from conical to planar. The homeotropic and planar textures correspond to the I and F phases, and the intermediate conical texture to the L phase. The polar angle of the surface tilt corresponds to the angle θ_-; the azimuthal angle of the surface tilt is an additional degree of freedom with no analogue in our theory. The surface tilt-angle transitions have been modeled by a potential similar to Eq. (1.1).

We can extend our mean-field theory by considering higher-order Fourier coefficients in the potential $V(\theta_-)$. First, consider nonzero h_{18}. If $h_{12} < -6|h_{18}|$, there is a pair of second-order transitions as above. If $h_{12} > 2|h_{18}|$,

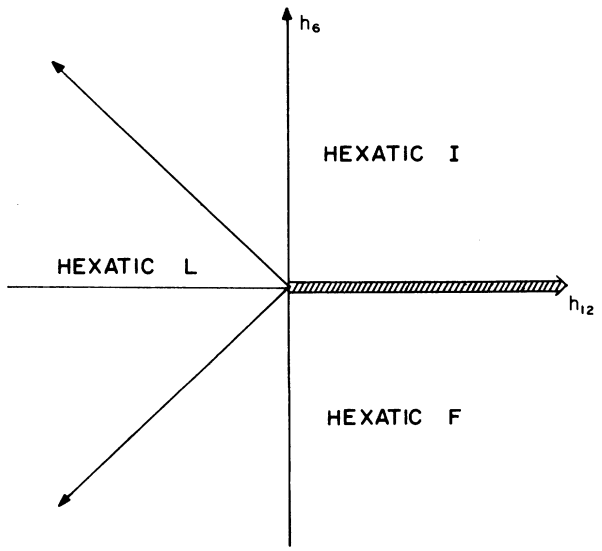

FIG. 3. Mean-field phase diagram as a function of h_6 and h_{12}. The double lines represent first-order and the single lines second-order transitions.

there is a direct first-order *I-F* transition. If $-6|h_{18}|<h_{12}<2|h_{18}|$ and $h_{18}>0$, there is a first-order *I-L* transition followed by a second-order *L-F* transition. Likewise, if $-6|h_{18}|<h_{12}<2|h_{18}|$ and $h_{18}<0$, there is a second-order *I-L* transition followed by a first-order *L-F* transition. Next, consider nonzero $h_{24},h_{30},\ldots$. If these terms are sufficiently large, there may be several *L* phases and several first-order transitions among these phases. However, we would be surprised if $V(\theta_-)$ contains this much fine structure.

IV. RENORMALIZATION-GROUP ANALYSIS

To go beyond mean-field theory, we must consider fluctuations in $\theta_-(\mathbf{r})$. The effect of these fluctuations depends on dimension. In a 3D stacked tilted hexatic system with many interacting layers, fluctuations produce only small corrections to the mean-field theory discussed above. Fluctuations are not expected to change the topology of the mean-field phase diagram of Fig. 3, although they may change the shape of the second-order lines near the "multicritical point" at $h_6=h_{12}=0$. If $h_{12}>0$, fluctuations have no major effects on the first-order *I-F* transition. If $h_{12}<0$, they reduce the critical values $|h_6^{IL}|$ and $|h_6^{LF}|$, and they change the exponent β in Eqs. (3.1) and (3.2) to $\beta\approx 0.31$, the value for the 3D Ising model. By contrast, in a 2D system fluctuations in $\theta_-(\mathbf{r})$ may qualitatively violate mean-field theory and can change the topology of the phase diagram of Fig. 3. The films studied by Dierker and Pindak[3] are only five layers thick, and hence are effectively 2D. Likewise, the L_β phases studied by Smith *et al.*[1] exhibit no correlations across bilayers, and hence may also be effectively 2D. To understand these experiments, we must assess the significance of fluctuations in 2D by using the renormalization group.

In our renormalization-group calculation, we follow the method of Kogut.[11] We work to second order in the potential $V(\theta_-)$ and use smooth momentum-space slicing. We impose a momentum-space ultraviolet cutoff $\Lambda=a^{-1}$, where a is a typical intermolecular spacing. In the renormalization-group transformation, we integrate out the high-momentum components of θ in the smoothly defined range from $e^{-l}\Lambda$ to Λ and then rescale distances by a factor of e^l. In our notation h_{6n} and K_- (with no explicit l dependence) are the initial coefficients at $l=0$, and $h_{6n}(l)$ and $K_-(l)$ are the effective coefficients at the length scale $e^l a$. For a general $V(\theta_-)$ of the form in Eq. (2.2), we obtain the differential recursion relations

$$\frac{dh_{6n}(l)}{dl}=\left[2-\frac{9n^2}{\pi K_-(l)}\right]h_{6n}(l)+\frac{9\alpha_1}{K_-(l)\Lambda^2}\left[\sum_{|j-m|=n}jmh_{6j}(l)h_{6m}(l)-\sum_{j+m=n}jmh_{6j}(l)h_{6m}(l)\right], \tag{4.1a}$$

$$\frac{dK_-(l)^{-1}}{dl}=-\sum_{n=1}^{\infty}\frac{162\alpha_2 n^4 h_{6n}(l)^2}{K_-(l)^3\Lambda^4}, \tag{4.1b}$$

where α_1 and α_2 are positive constants of order 1 that depend on the details of the momentum-slicing procedure.[11] Szeto and Dresselhaus[12] have derived similar recursion relations for two symmetry-breaking fields using a different method.

The recursion relations (4.1) have terms at first and second order in the h's. If we consider only the first-order terms, then K_- is a constant of the renormalization group, and h_{6n} is relevant for $K_->K_{c,6n}$, where $K_{c,6n}=9n^2/2\pi$. If we include the second-order terms, then $K_-(l)$ increases with increasing l, and hence the critical *initial* stiffnesses are $K_{c,6n}\lesssim 9n^2/2\pi$. The critical initial stiffnesses $K_{c,6n}$ are nonuniversal because they depend on all the relevant and irrelevant h's. The corrections to $K_{c,6n}$ are of order $V/K_-\Lambda^2$. Two critical stiffnesses, $K_{c,6}$ and $K_{c,12}$, are particularly important to our theory. At $K_-=K_{c,6}\lesssim 9/2\pi$, there is a "lock-in" transition[13] above which h_6 is relevant and $M_-\equiv\langle e^{6i\theta_-}\rangle$ acquires long-range order. Similarly, if $h_6=0$, there is a lock-in transition at $K_-=K_{c,12}\lesssim 18/\pi$, above which h_{12} is relevant and $\langle e^{12i\theta_-}\rangle$ acquires long-range order. The value of $K_{c,6}$ at $h_6=0$ should be close to $9/2\pi$ because it is only renormalized by h_{12} and higher-order irrelevant variables. Likewise, the value of $K_{c,12}$ at $h_6=h_{12}=0$ should be close to $18/\pi$ because it is only renormalized by h_{18} and higher-order irrelevant variables.

Note that $h_{18},h_{24},\ldots$, only become relevant at stiffnesses much higher than the stiffnesses at which h_6 and h_{12} become relevant. Even if they are relevant, $h_{18}(l),h_{24}(l),\ldots$, grow less rapidly than $h_6(l)$ and $h_{12}(l)$. For this reason, the higher-order coefficients can affect the physics only in the very small region of the phase diagram where h_6 and h_{12} are initially both small. We therefore neglect the higher-order coefficients and consider only the h_6 and h_{12} terms. We truncate the set of recursion relations (4.1) to obtain

$$\frac{dh_6(l)}{dl}=\left[2-\frac{9}{\pi K_-(l)}\right]h_6(l)+\frac{36\alpha_1 h_6(l)h_{12}(l)}{K_-(l)\Lambda^2}, \tag{4.2a}$$

$$\frac{dh_{12}(l)}{dl}=\left[2-\frac{36}{\pi K_-(l)}\right]h_{12}(l)-\frac{9\alpha_1 h_6(l)^2}{K_-(l)\Lambda^2}, \tag{4.2b}$$

$$\frac{dK_-(l)^{-1}}{dl}=-\frac{162\alpha_2}{K_-(l)^3\Lambda^4}[h_6(l)^2+16h_{12}(l)^2]. \tag{4.2c}$$

If $K_->K_{c,6}$, an initially small value of $|h_6|$ increases with increasing length scale. If $K_->K_{c,12}$, an initially small value of $|h_{12}|$ also increases. When $l=l^*$ such that $\max[|h_6(l^*)|,|h_{12}(l^*)|]=O(K_-\Lambda^2)$, our expansion in powers of $V(\theta_-)$ ceases to be valid. At this length scale we must match directly onto an approximation that is valid for *large* $V(\theta_-)$. The renormalized potential at this length scale, $V_{l^*}(\theta_-)$, consists of a series of "valleys" separated by high energy barriers. Fluctuations in θ_- are

then confined to one valley. Four types of behavior are possible.

(1) If $K_- > K_{c,12}$, both h_6 and h_{12} are relevant. If $h_{12} < 0$, $V_{l^*}(\theta_-)$ consists of a series of valleys with Ising-type internal structure, as in Fig. 1. Because θ_- is confined to one valley, our problem is equivalent to a 2D continuum Ising model with fluctuations. We therefore obtain second-order, Ising-type *I-L* and *L-F* transitions. If we neglect fluctuations in the Ising model, these transitions occur when $h_6(l^*) = \pm 4|h_{12}(l^*)|$; with fluctuations they occur at a reduced value of $|h_6(l^*)|$.

Using the nonlinear recursion relations (4.2), we can find the critical initial values of h_6 in two limits. First, in the limit $K_- \to \infty$, the recursion relations can be integrated trivially. We find the second-order transitions at $h_6^{IL} = -h_6^{LF} = 4|h_{12}|$, just as in mean-field theory. This result is not surprising, because in the limit $K_- \to \infty$ all fluctuations between and within the valleys of $V(\theta_-)$ are quenched.

Next, consider the limit $K_- \to K_{c,12}^+$. We assume that in this limit $|h_6| \ll |h_{12}|$ near the second-order transitions; we will later show that this ansatz is self-consistent. We therefore neglect the $h_6(l)^2$ terms in (4.2b) and (4.2c). We also neglect the $h_6(l)h_{12}(l)$ term in (4.2a) because we iterate only until $h_{12}(l)$ grows to $O(K_- \Lambda^2)$. We therefore obtain the approximate recursion relations,

$$\frac{dh_6(l)}{dl} = \left[2 - \frac{9}{\pi K_-(l)}\right] h_6(l) , \tag{4.3a}$$

$$\frac{dh_{12}(l)}{dl} = \left[2 - \frac{36}{\pi K_-(l)}\right] h_{12}(l) , \tag{4.3b}$$

$$\frac{dK_-(l)^{-1}}{dl} = -\frac{2592\alpha_2 h_{12}(l)^2}{K_-(l)^3 \Lambda^4} . \tag{4.3c}$$

These recursion relations have a fixed point at $h_6 = h_{12} = 0$ and $K_- = 18/\pi$. We linearize about this fixed point and solve the linearized equations by the method of Kosterlitz.[14] Figure 4 shows the resulting renormalization-group flows in the (h_{12}, K_-^{-1}) plane. The incoming separatrices give $K_{c,12}^{-1}$ as a function of h_{12},

$$K_{c,12}^{-1} = \frac{\pi}{18} + \frac{\pi^2 \sqrt{\alpha_2}|h_{12}|}{9\Lambda^2} . \tag{4.4}$$

We begin at the point labeled A. The renormalization-group trajectory is given by

$$h_6(l) = h_6 \exp\left[\frac{3l}{2}\right] , \tag{4.5a}$$

$$h_{12}(l) = -\frac{\Lambda^2 C}{4\pi\sqrt{\alpha_2}} \csc(Cl + D) , \tag{4.5b}$$

$$K_-(l)^{-1} = \frac{\pi}{18} + \frac{\pi C}{36} \cot(Cl + D) , \tag{4.5c}$$

where

$$C^2 \approx \frac{8\pi^2 \sqrt{\alpha_2}|h_{12}|(K_- - K_{c,12})}{9\Lambda^2} , \tag{4.6a}$$

$$\sin D = \frac{\Lambda^2 C}{4\pi\sqrt{\alpha_2}|h_{12}|} . \tag{4.6b}$$

We iterate until we reach the length scale l^* given by $|h_{12}(l^*)| = O(K_- \Lambda^2)$. Equations (4.5) and (4.6) give

$$l^* \approx \frac{\pi}{C} . \tag{4.7}$$

At that length scale $h_{16}(l)$ grows to

$$h_6(l^*) \approx h_6 \exp\left[\frac{3\pi}{2C}\right] . \tag{4.8}$$

Because the critical values of $h_6(l^*)$ are approximately $\pm 4|h_{12}(l^*)|$, with small corrections for fluctuations, the critical initial values of h_6 are given by

$$h_6^{IL} = -h_6^{LF} \approx K_- \Lambda^2 \exp\left[-\frac{3\pi}{2C}\right] \approx K_- \Lambda^2 \exp\left[-\left[\frac{81\Lambda^2}{32\sqrt{\alpha_2}|h_{12}|(K_- - K_{c,12})}\right]^{1/2}\right] \tag{4.9}$$

as $K_- \to K_{c,12}^+$. Near the transitions, $|h_6(l)| \ll |h_{12}(l)|$ for all $l < l^*$, thus confirming our ansatz.

(2) If $K_- > K_{c,12}$ and $h_{12} > 0$, both h_6 and h_{12} are again relevant. In this case $V_{l^*}(\theta_-)$ may have valleys at $\theta_- = 0°$ (mod 60°) and 30° (mod 60°), as in Fig. 2. If $h_6 > 0$, the valleys at $\theta_- = 0°$ (mod 60°) are deeper, and θ_- fluctuates inside one of those valleys, in the I phase. If $h_6 < 0$, the valleys at $\theta_- = 30°$ (mod 60°) are deeper, and θ_- fluctuates in the F phase. As h_6 passes through 0, there is a first-order *I-F* transition.

(3) If $K_{c,6} < K_- < K_{c,12}$, then h_6 is relevant but h_{12} is irrelevant. If the initial value of h_6 is small, the potential $V(\theta_-)$ iterates to $V_{l^*}(\theta_-) = -h_6(l^*)\cos 6\theta_-$. If $h_6 > 0$, θ_- fluctuates in the I phase, and if $h_6 < 0$, θ_- fluctuates in the F phase. If $h_6 = 0$, then $V(\theta_-)$ iterates to 0, and our problem becomes a 2D xy model with no symmetry-breaking field. In that case there is no long-range order in θ_-. We therefore obtain a second-order rather than a first-order *I-F* transition as h_6 passes through 0. The line of critical points at $h_6 = 0$ for $K_{c,6} < K_- < K_{c,12}$ is a fluctuation effect, peculiar to two dimensions.[13]

(4) If $K_- < K_{c,6}$, then h_6 and h_{12} are both irrelevant. The potential $V(\theta_-)$ then iterates to 0, and there is no long-range order in θ_-. We therefore obtain the unlocked tilted hexatic phase studied by Nelson and Halperin.[2] In this phase $\theta(\mathbf{r})$ and $\phi(\mathbf{r})$ fluctuate independently.

By combining the behaviors in regimes (1)–(4), we obtain a phase diagram in the initial parameters h_6, h_{12},

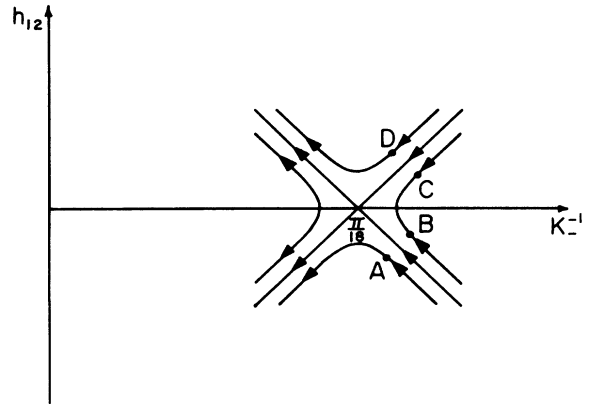

FIG. 4. Renormalization-group flows in the (h_{12},K_-^{-1}) plane for $h_6=0$. The points labeled $A-D$ are discussed in the text.

and K_-^{-1}. Figure 5 presents two cross sections of that phase diagram for fixed positive and negative h_{12}. For $K_- \to \infty$ mean-field theory is valid, because in that limit all fluctuations are quenched. For $K_- > K_{c,12}$, the phase diagram depends on the sign of h_{12}. If $h_{12}<0$, the phase diagram shows I, L, and F phases with second-order, Ising-type I-L and L-F transitions. The L phase boundaries come together at $K_- = K_{c,12}$ with an essential singularity as in Eq. (4.9). If $h_{12}>0$, the phase diagram

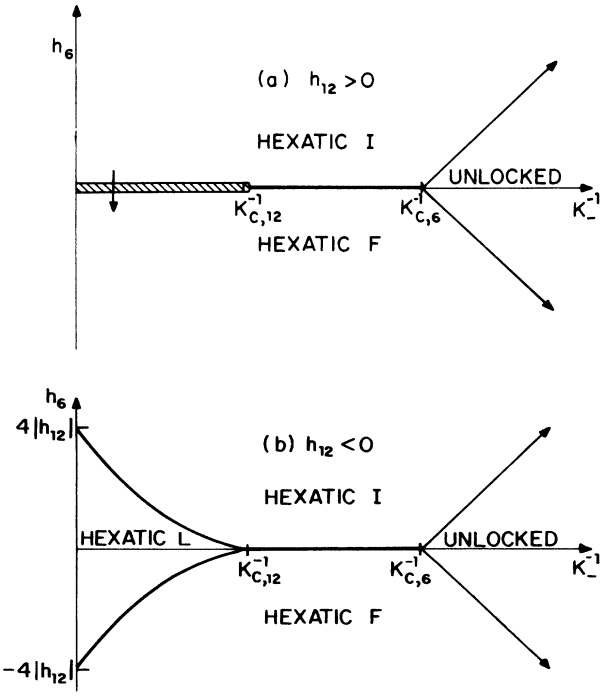

FIG. 5. Two cross sections of the theoretical phase diagram, for (a) constant $h_{12}>0$ and (b) constant $h_{12}<0$, as a function of h_6 and the temperaturelike variable K_-^{-1}. The double lines represent first-order transitions and the single lines second-order transitions. The arrow in (a) indicates the approximate position of the I-F transition in Ref. 3.

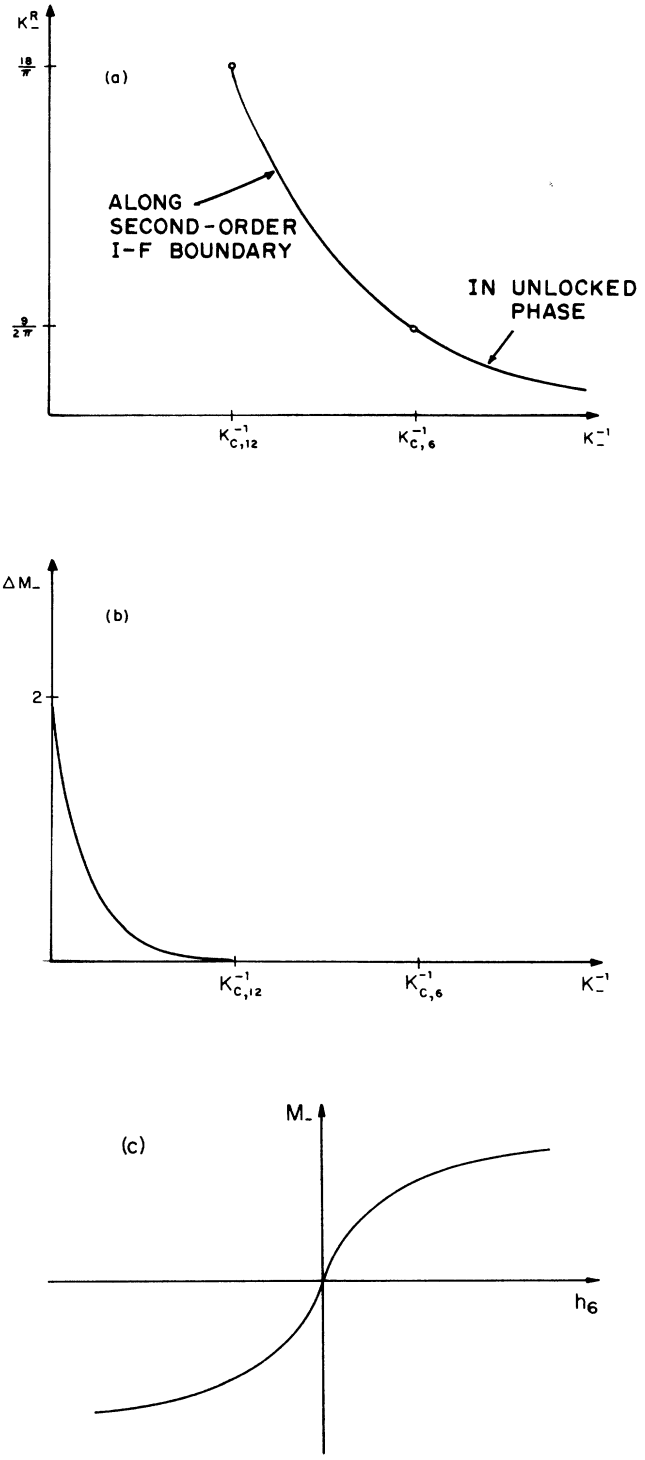

FIG. 6. (a) The renormalized θ_- stiffness constant K_-^R as a function of the temperaturelike variable K_-^{-1}, for $h_6=0$ and fixed $h_{12}\neq 0$. Universal limits at $K_{c,6}$ and $K_{c,12}$ are shown. K_-^R approaches its universal value at $K_{c,12}$ with a square-root cusp (see Ref. 13). (b) The discontinuity ΔM_- across the first-order I-F transition as a function of K_-^{-1}. (c) The order parameter M_- as a function of h_6 near the second-order I-F transition, for $K_{c,6}<K_-<K_{c,12}$.

shows a first-order *I-F* transition, which now ends in a tricritical point at $K_- = K_{c,12}$. For $K_{c,6} < K_- < K_{c,12}$, both cross sections of the phase diagram show a direct, second-order *I-F* transition. For $K_- < K_{c,6}$, both cross sections show the unlocked phase.

We define the renormalized θ_- stiffness constant as

$$K_-^R \equiv \lim_{l\to\infty} K_-(l) \ . \tag{4.10}$$

The behavior of K_-^R as a function of the initial stiffness K_- is shown in Fig. 6(a). Although the critical initial stiffnesses $K_{c,6}$ and $K_{c,12}$ are nonuniversal, the renormalized stiffness K_-^R has some universal limits. Along the second-order *I-F* phase boundary, for $h_6 = 0$ and $K_{c,6} < K_- < K_{c,12}$, Eqs. (4.2) imply the universal results

$$\lim_{K_- \to K_{c,12}^-} K_-^R = \frac{18}{\pi} \ , \tag{4.11a}$$

$$\lim_{K_- \to K_{c,6}^+} K_-^R = \frac{9}{2\pi} \ . \tag{4.11b}$$

Similarly, in the unlocked phase, for $K_- < K_{c,6}$ and all values of h_6, we find

$$\lim_{K_- \to K_{c,6}^-} K_-^R = \frac{9}{2\pi} \ . \tag{4.12}$$

The limit (4.11a) can be derived by examining the renormalization-group flows beginning at points such as *B* and *C* in the (h_{12}, K_-^{-1}) plane of Fig. 4. The limits (4.11b) and (4.12) can be derived by examining flows in the (h_6, K_-^{-1}) plane near the fixed point $h_6 = h_{12} = 0$ and $K_- = 9/2\pi$.

Now consider the order parameter M_-. We make the scaling ansatz

$$M_-(h_6(l), h_{12}(l), K_-(l)) = e^{\omega \delta l} M_-(h_6(l+\delta l), h_{12}(l+\delta l), K_-(l+\delta l)) \tag{4.13}$$

for $\delta l \ll 1$. For small $h_6(l)$ and $h_{12}(l)$, we find

$$\omega = -\frac{9}{\pi K_-(l)} \ . \tag{4.14}$$

By integrating (4.13), we obtain the scaling relation

$$M_-(h_6, h_{12}, K_-) = \exp\left[-\int_0^l dl' \frac{9}{\pi K_-(l')} \right] M_-(h_6(l), h_{12}(l), K_-(l)) \ . \tag{4.15}$$

It is interesting to consider the behavior of M_- in each of the four regimes discussed above.

(1) If $K_- > K_{c,12}$ and $h_{12} < 0$, there are second-order *I-L* and *L-F* transitions, and the *L* phase is characterized by $\mathrm{Im} M_- \neq 0$. Near the transitions, $\mathrm{Im} M_-$ follows the power laws (3.1) and (3.2). Because of fluctuations within the valleys of $V(\theta_-)$, the exponent β becomes $\frac{1}{8}$, the value for the 2D Ising model.

(2) If $K_- > K_{c,12}$ and $h_{12} > 0$, there is a first-order *I-F* transition, across which M_- has a finite discontinuity ΔM_-. We are interested in the behavior of ΔM_- near the tricritical point at $K_{c,12}$. Consider an infinitesimal h_6 above or below the first-order transition. We again use the recursion relations (4.3). We begin at the point labeled *D* in Fig. 4 and iterate up to the length scale l^* given by Eq. (4.7), where $h_{12}(l^*) = O(K_- \Lambda^2)$. The scaling relation (4.15) then implies

$$\Delta M_-(h_{12}, K_-) = \exp\left[-\int_0^{l^*} dl \frac{9}{\pi K_-(l)} \right] \Delta M_-(h_{12}(l^*), K_-(l^*)) \ . \tag{4.16}$$

Because $h_{12}(l^*)$ is large, $\Delta M_-(h_{12}(l^*), K_-(l^*))$ is of order 1. In the integral we approximate $K_-(l) \approx 18/\pi$. We therefore obtain

$$\Delta M_-(h_{12}, K_-) \approx \exp\left[-\frac{l^*}{2} \right] \approx \exp\left[-\left[\frac{9\Lambda^2}{32\sqrt{\alpha_2}|h_{12}|(K_- - K_{c,12})} \right]^{1/2} \right] \ . \tag{4.17}$$

At the tricritical point, ΔM_- vanishes with an essential singularity, as in Fig. 6(b).

(3) If $K_{c,6} < K_- < K_{c,12}$, then h_{12} is irrelevant, and there is a second-order *I-F* transition at $h_6 = 0$. We are interested in the way M_- vanishes as $h_6 \to 0$. Using the recursion relations (4.2), we begin with h_6 small and iterate up to the length scale l^* where $|h_6(l^*)| = O(K_- \Lambda^2)$. A characteristic value for $K_-(l)$ during the iteration is K_-^R. We therefore obtain

$$l^* \approx \left[\frac{\pi K_-^R}{2\pi K_-^R - 9} \right] \ln\left[\frac{K_-^R \Lambda^2}{|h_6|} \right] \ . \tag{4.18}$$

At this length scale, $|M_-(h_6(l^*), K_-(l^*))|$ is of order 1. The scaling relation (4.15) then implies

$$|M_-(h_6, K_-)| \propto |h_6|^{9/(2\pi K_-^R - 9)} \tag{4.19}$$

near the second-order transition. This power law is illustrated in Fig. 6(c).

(4) If $K_- < K_{c,6}$, then $M_- = 0$ in the unlocked phase. The behavior of M_- near the *I*-unlocked and *F*-unlocked transitions has already been studied.[13] At the boundary of the unlocked phase, M_- vanishes with an essential singularity.

So far we have considered an infinite system. If the system has a finite size L, we cannot iterate to any length scale greater than L. Rather, we must cut off the iteration at

$$l^* = \ln\left[\frac{L}{a}\right] . \tag{4.20}$$

At this length scale, θ_- has only one unintegrated degree of freedom, the zero-momentum mode. We can then use mean-field theory in this mode. Neither $h_6(l)$ nor $h_{12}(l)$ can iterate all the way to 0 by the time l reaches l^*. Both Fourier coefficients can therefore affect the phase transitions. Szeto and Dresselhaus[15] have studied finite-size effects in the 2D xy model using a similar argument.

In a finite system, if $h_{12}<0$, there is a small wedge of the L phase for all K_-. Because the I-L and L-F transitions occur at $h_6(l^*)=\pm 4|h_{12}(l^*)|$, the critical initial values of h_6 are

$$h_6^{IL} = -h_6^{LF} = 4|h_{12}|\left[\frac{L}{a}\right]^{-27/\pi K_-} , \tag{4.21}$$

or the infinite-system values, whichever are larger. If $h_{12}>0$, the I-F transition is at least weakly first-order, with a nonzero discontinuity ΔM_-, for all K_-. To find this discontinuity, we use the scaling relation (4.16). Even if $h_{12}(l^*)$ is very small, $\Delta M_-(h_{12}(l^*),K_-(l^*))$ is of order 1, because in a finite system there is only one θ_- mode at this length scale. We therefore obtain the discontinuity

$$\Delta M_-(h_{12},K_-) \approx \left[\frac{L}{a}\right]^{-9/\pi K_-} , \tag{4.22}$$

or the infinite-system value, whichever is larger. In writing Eqs. (4.21) and (4.22), we assume that $K_-(l)$ does not change much from $l=0$ to l^*, and hence we use the initial value to estimate the exponents.

V. DISCUSSION OF PHASE DIAGRAM

In order to compare our theory with experiments, we must examine two details about the Hamiltonian (2.1). First, consider the effect of elastic anisotropy. In the Hamiltonian (2.1), we assume that all the stiffnesses are isotropic. However, on a microscopic length scale K_1 and g are really anisotropic tensors with eigenvalues K_1^B, K_1^S, g^B, and g^S, corresponding to bend and splay, i.e., variations parallel and perpendicular to the local tilt direction, respectively. The stiffness K_6 is always isotropic because of the local hexagonal symmetry. When we change variables from θ and ϕ to θ_+ and θ_-, the acoustic "polarization" constants α and β depend on the wave-vector direction in reciprocal space (just as ordinary phonon polarization constants depend on wave-vector direction in anisotropic media). In general, K_- will also depend on the wave-vector direction in a complicated way. However, in the physically realistic limit $K_6 \gg K_1^B$, K_1^S, g^B, and g^S, one can show that K_- reduces to the tensor K_1. Nelson and Pelcovits[16] have shown that the tensor K_1 becomes isotropic at long length scales. By a straightforward application of their recursion relations (4.8) and (4.9), one can show that K_1^B and K_1^S both evolve toward their arithmetic mean $(K_1^B+K_1^S)/2$. For that reason, on long length scales we can use the asymptotic value $(K_1^B+K_1^S)/2$ in place of K_- in the recursion relations.

Next, consider how the phase diagrams of this paper are modified if the membrane is crystalline rather than hexatic. To be sure, recent theoretical work[6,17] has shown that the free energy of an unbound dislocation is negative for all $T>0$ in any 2D membrane that can buckle out of the plane. This result indicates that 2D crystalline phases cannot be in equilibrium for any $T>0$, and that the hexatic phases are preferred. However, the experiments of Smith *et al.*[1] do not actually determine whether their $L_{\beta'}$ phases are crystalline or hexatic. The dislocations could have very large core energies, in which case the dislocation density would be very low and the positional correlation length could be greater than experimental length scales. Furthermore, interlayer interactions could prevent the dislocations from buckling. Just in case the $L_{\beta'}$ phases are crystalline, we consider how crystalline order affects the results of this paper.

In a crystalline membrane, K_6 becomes infinite, and $\theta(\mathbf{r})$ is replaced by the fixed orientation θ_0 of the crystal axes. In the Hamiltonian, we must now include the coupling of $\phi(\mathbf{r})$ to the lattice strain field $u_{ij}(\mathbf{r})$. Nelson and Halperin[2] argue that the Hamiltonian for a crystalline membrane becomes

$$\frac{H}{k_B T} = \int d^2\mathbf{r}[\mu u_{ij}^2 + \tfrac{1}{2}\lambda u_{kk}^2 + \tfrac{1}{2}K_1|\nabla\phi|^2 + w(u_{ij}-\tfrac{1}{2}\delta_{ij}u_{kk})s_i s_j + V(\theta_0-\phi)] , \tag{5.1}$$

where $\mathbf{s}\equiv(\cos\phi, \sin\phi)$. By generalizing their argument to $h_{12}\neq 0$, one can show that the crystalline analogues of I, L, and F are all stable phases. However, if $w\neq 0$ then the state with $M_-=0$ becomes unstable. The coupling w is relevant for $K_1 \gtrsim 1/\pi$. For that reason, w destabilizes the unlocked phase and the second-order I-F transition. Although our mean-field theory should be a useful guide to transitions among the crystalline analogues of I, L, and F phases, our renormalization-group analysis does not apply to these transitions. We still expect, however, either a first-order I-F transition or a pair of Ising-type, second-order I-L and L-F transitions for large K_1.

Dierker and Pindak's observation[3] of a weakly first-order I-F transition in five-layer thermotropic liquid-crystal films fits into our theoretical phase diagram. From Fig. 5(a), we expect a first-order transition if $h_{12}>0$ and $K_- \geq K_{c,12} \approx 18/\pi$. Dierker and Pindak indirectly determine the value of K_- at light-scattering length scales. Their experiments measure K_1^B and K_1^S in the smectic-C phase of a two-layer film. By extrapolating K_1^B and K_1^S from the smectic-C phase into the hexatic-I phase, we can estimate those values in the hexatic-I phase. From their Fig. 1(a) we estimate $K_1^S \approx 70/\pi$ and $K_1^B \approx 10/\pi$ (when normalized by $k_B T$). The mean, which plays the role of K_- on long length scales, is $K_-^{\text{eff}} = (K_1^B+K_1^S)/2 \approx 40/\pi$. Because elasticities are roughly proportional to film thickness, we expect

$K_{-}^{\text{eff}} \approx 100/\pi$ in five-layer films. That value is indicated by the arrow on our Fig. 5(a). It is well within the first-order *I-F* transition region. Equation (4.17) shows that the discontinuity in M_{-} increases very slowly with K_{-} if the microscopic $h_{12} \ll \Lambda^2$. It is therefore not surprising that the observed *I-F* transition is only very weakly first-order. Our theory predicts that this transition will be more strongly first-order in systems with higher tilt elasticities. It also implies that there will be a tricritical point in systems where $(K_1^B + K_1^S)/2$ is reduced to approximately $18/\pi$. However, the finite-size effects discussed in Sec. IV will smear out this tricritical point.

Dierker and Pindak have used light scattering to measure the optical-mode relaxation rate Γ_{-}. This relaxation rate is proportional to the restoring force at the minimum of $V(\theta_{-})$, which is

$$18|h_6(l_0)| + 72h_{12}(l_0) \ . \tag{5.2}$$

In this expression, h_6 and h_{12} must be evaluated at $l_0 = \ln(\lambda/a)$, where λ is the inverse of the wave-vector transfer. By linearizing the recursion relations (4.2), we obtain

$$h_6(l_0) \approx h_6 \left[\frac{\lambda}{a}\right]^{2-9/\pi K_{-}} , \tag{5.3a}$$

$$h_{12}(l_0) \approx h_{12} \left[\frac{\lambda}{a}\right]^{2-36/\pi K_{-}} . \tag{5.3b}$$

Close to the *I-F* transition, we can write $h_6 \propto (T - T_{IF})$, and hence (assuming no singularities in the dynamics of this first-order transition),

$$\Gamma_{-} \propto |T - T_{IF}| + \text{const} \ . \tag{5.4}$$

The value of Γ_{-} at the transition is proportional to $h_{12}(l_0)$. This value should increase with increasing tilt elasticities.

The experiments on $L_{\beta'}$ phases by Smith *et al.*[1] also fit into our theoretical phase diagram, no matter whether these phases are hexatic or crystalline. If these phases are hexatic, then Fig. 5(b) shows that the intermediate $L_{\beta L}$ phase should be present, and that the $L_{\beta I}$-$L_{\beta L}$ and $L_{\beta F}$-$L_{\beta L}$ transitions should be second order, provided that $h_{12} < 0$ and $K_{-} \geq K_{c,12} \approx 18/\pi$. If these phases are crystalline, then we expect second-order $L_{\beta I}$-$L_{\beta L}$ and $L_{\beta F}$-$L_{\beta L}$ transitions whenever $h_{12} < 0$ and K_1 is large. To test our predictions, one should analyze the line shapes to determine whether these phases are hexatic or crystalline, and one should measure $K_{-}^{\text{eff}} = (K_1^B + K_1^S)/2$ in these phases.

There are three basic microscopic questions for a theory of hexatic-to-hexatic transitions. First, the theory must explain in which direction h_6 changes sign as a function of temperature in thermotropics and lyotropics. Second, it must explain in which direction h_6 changes sign as a function of humidity in lyotropics. Third, it must account for the sign of h_{12} at the transitions.

In both thermotropics and lyotropics. the *I* phase is the higher-temperature phase and the *F* phase is the lower-temperature phase. This observed sequence implies that h_6 changes sign from positive to negative as T decreases. Sirota[18] has developed a microscopic model for a general liquid-crystal phase sequence, which includes the *I* and *F* phases. In this model *F* is the lowest-energy, lowest-entropy phase, and *I* is a higher-energy, higher-entropy phase, in agreement with experiment. The basic assumption of this model is that intermolecular "tilt-bonds" have a much lower energy than "flat-bonds," which in turn have a much lower energy than "double-tilt bonds." This basic assumption about bond energies is only justified by the known structure of the lowest-temperature phase. Before this model can be a conclusive explanation of the phase sequence, that assumption must be justified on a more fundamental, chemical basis, perhaps using a theoretical intermolecular potential.

Among the $L_{\beta'}$ phases, the $L_{\beta I}$ phase is the higher-humidity phase and the $L_{\beta F}$ phase is the lower-humidity phase, which implies that h_6 changes sign from positive to negative as humidity decreases. The major effect of humidity is to increase the layer spacing, and hence to allow the layers to fluctuate more. For that reason, higher humidity should favor the higher-entropy phase, in which the layers are more disordered and need more room to fluctuate. The higher-humidity phase should therefore be the same as the higher-temperature phase. If Sirota's model is successful as an explanation of the phase sequence in temperature, it will also be successful as an explanation of the phase sequence in humidity.

We do not yet have any microscopic explanation of why $h_{12} > 0$ in the thermotropics studied by Dierker and Pindak and why $h_{12} < 0$ in the lyotropics studied by Smith *et al.* We cannot even be certain that h_{12} will have these signs in all thermotropics or all lyotropics. To understand the sign of h_{12}, one must use some theoretical intermolecular potential to calculate the free energy of a lattice of tilted hexatic molecules as a function of θ_{-}, and then project out the $\cos(12\theta_{-})$ Fourier component. We do not know of any calculations of an intermolecular potential for thermotropics or lyotropics that can yield this information.

VI. THE STAR DEFECT

Dierker, Pindak, and Meyer[5] have discovered a remarkable textural defect in thin tilted hexatic films. In this section we discuss their theory for this defect inside the *I* or *F* phase and point out the significance of the acoustic polarization constants α and β of Eq. (2.3a). We then predict the behavior of this defect close to the *I-F*, *I-L*, and *L-F* transitions.

Thin liquid-crystal films can be drawn in the smectic-*C* phase. In this phase there are quasi-long-range correlations in both $\phi(\mathbf{r})$ and $\theta(\mathbf{r})$, but the magnitude of the order in $\theta(\mathbf{r})$ [which is induced by the order in $\phi(\mathbf{r})$] is very small.[2] When a film is formed, it can have a vortex about which $\phi(\mathbf{r})$ goes through an angle of 2π. If the sample is cooled into the hexatic-*I* phase, the magnitude of the bond-orientational order becomes much greater, and $\theta(\mathbf{r})$ is locked to $\phi(\mathbf{r})$ by the h_6 term in the Hamiltonian. The 2π vortex in $\phi(\mathbf{r})$ therefore becomes a 2π disclination in $\theta(\mathbf{r})$. To reduce its energy, this defect can break up into

the N-armed star structure shown in Fig. 7. At the end of each arm, there is a disclination of angle $2\pi/6$ in $\theta(\mathbf{r})$. At the center, there is a disclination of angle $2\pi(1-N/6)$ in $\theta(\mathbf{r})$ and a vortex of angle 2π in $\phi(\mathbf{r})$. Figure 7 shows the case $N=5$, which is the only case that has actually been observed so far. We consider nonchiral materials or racemic mixtures, in which the arms are straight. In chiral materials, the arms have a spiral structure.[5]

We can study this defect by changing variables from $\theta(\mathbf{r})$ and $\phi(\mathbf{r})$ to $\theta_+(\mathbf{r})$ and $\theta_-(\mathbf{r})$. Note that $\theta_+(\mathbf{r})$ and $\theta_-(\mathbf{r})$ are uniquely defined only in a simply connected region that does not contain a vortex or disclination. Each arm has length R and width $\xi \ll R$. Across each arm $\theta_-(\mathbf{r})$ jumps by $2\pi/6$, but $\theta_+(\mathbf{r})$ does not make any sudden jumps. Therefore, across each arm $\phi(\mathbf{r})$ jumps by $2\pi\alpha/6$ and $\theta(\mathbf{r})$ jumps by $-2\pi\beta/6$. In the physically realistic limit $K_6 \gg K_1$ and g, we have $\beta=1-\alpha\ll 1$, and hence $\theta(\mathbf{r})$ jumps very little across each arm. In the wedge of angle $2\pi/N$ between two arms, $\theta_-(\mathbf{r})$ is constant and $\theta(\mathbf{r})$, $\phi(\mathbf{r})$, and $\theta_+(\mathbf{r})$ all advance by $(2\pi/N)(1-\alpha N/6)$.

Following Ref. 5, we calculate the energy of a star defect at the origin relative to the energy of a single vortex and disclination of angle 2π at the origin. Suppose that each arm has energy ε per unit length (normalized by k_BT). In polar coordinates (r,Θ) the Hamiltonian (2.4) implies

$$\frac{\Delta E}{k_BT}=\frac{K_+N}{2}\int_{-\pi/N}^{\pi/N}d\Theta\int_a^\infty r\,dr(|\nabla\theta_+^{\text{star}}|^2-|\nabla\theta_+^{\text{no star}}|^2)+\varepsilon RN\ . \tag{6.1}$$

This integral excludes the cores of radius a about the defects at the origin and the ends of the arms.[19] We find the minimum-energy configuration $\theta_+(r,\Theta)$ by solving Laplace's equation $\nabla^2\theta_+=0$ in the wedge $-\pi/N<\Theta<\pi/N$ subject to the boundary conditions

$$\theta_+(r,\pm\pi/N)=\begin{cases}\pm(\pi/N)(1-\alpha N/6) & \text{if } r<R\\ \pm\pi/N & \text{if } r>R\ .\end{cases} \tag{6.2}$$

We obtain

$$\frac{\Delta E}{k_BT}=-\frac{K_+\alpha N\pi}{36}(12-\alpha-\alpha N)\ln\frac{R}{a}+\varepsilon RN\ . \tag{6.3}$$

The minimum-energy arm length is obtained by minimizing with respect to R,

$$R=\frac{\alpha\pi}{36}(12-\alpha-\alpha N)\gamma a\ . \tag{6.4}$$

where $\gamma\equiv K_+/\varepsilon a$. The corresponding energy is

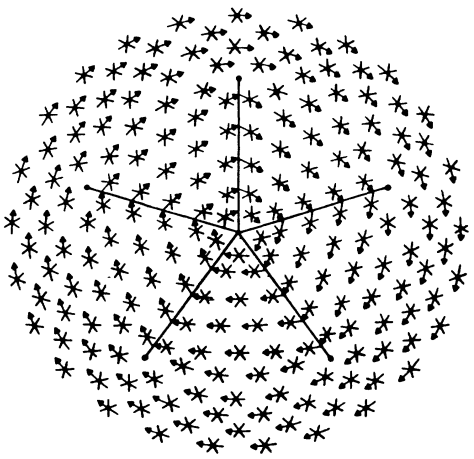

FIG. 7. Structure of the five-armed star defect in the I phase (from Ref. 5).

$$\frac{\Delta E}{k_BT}=-\frac{K_+\alpha N\pi}{36}(12-\alpha-\alpha N)\times\left[\ln\left[\frac{\alpha\pi}{36}(12-\alpha-\alpha N)\gamma\right]-1\right]\ . \tag{6.5}$$

A defect with $N=5$ minimizes the energy for $45\lesssim\gamma\lesssim(1.2)^{5/2\beta}$, and a defect with $N=6$ minimizes the energy for $\gamma\gtrsim(1.2)^{5/2\beta}$ So far only the five-armed star defect has been observed, but the six-armed star defect might be observed in a system in which β and γ are sufficiently large.

To find the arm width ξ and energy ε, consider a model of a single, isolated arm. In the thin-arm approximation $\xi\ll R$, we assume that the arm is infinite and uniform in the y direction and calculate the minimum-energy profile $\theta_-(x)$. From the Hamiltonian (2.4) we obtain

$$K_-\frac{d^2\theta_-}{dx^2}=\frac{dV}{d\theta_-}\ . \tag{6.6}$$

Inside the I phase, far from any transition, we can neglect all terms in $V(\theta_-)$ beyond the h_6 term. Equation (6.6) then becomes

$$K_-\frac{d^2\theta_-}{dx^2}=6h_6\sin[6\theta_-(x)]\ . \tag{6.7}$$

The boundary conditions are $\theta_-(-\infty)=0$ and $\theta_-(\infty)=2\pi/6$. This problem is a standard sine-Gordon soliton problem. The solution is

$$\theta_-(x)=\tfrac{1}{3}\cot^{-1}\left[-\sinh\frac{x}{\xi}\right]\ , \tag{6.8}$$

where

$$\xi=\tfrac{1}{6}\sqrt{K_-/h_6}\ . \tag{6.9}$$

From the Hamiltonian (2.4), the energy of the soliton per unit length is

$$\varepsilon=\tfrac{4}{3}\sqrt{K_-h_6}\ . \tag{6.10}$$

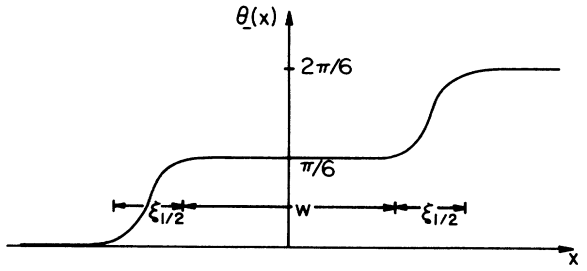

FIG. 8. Minimum-energy profile $\theta_-(x)$ across one arm in the I phase near the first-order I-F transition, for $0<h_6\ll h_{12}$. This profile can be viewed as two "half-arms" of width $\xi_{1/2}$ separated by a region of the F phase with width w.

The physics of this defect inside the F phase is the same.

As an aside, we note that θ_- defect lines also occur in another context, outside of the star defect.[20] A film in the I phase may contain distinct domains of, for example, $\theta_-=0$ and $\theta_-=\pi/3$. These domains are separated by a domain wall, across which θ_- increases by $\pi/3$. Similar domain walls can occur in the F phase. The physics of a θ_- domain wall is identical to the physics of an arm of a star defect. Our theory of a star-defect arms applies equally well to these domain walls.

Now suppose that a film containing a star defect or a θ_- domain wall is cooled toward the first-order I-F transition in a material with $h_{12}>0$. Near the transition h_6 becomes small, and we must consider the h_{12} term in Eq. (6.6). This equation has a simple analogy in classical mechanics: it describes the motion of a particle of mass K_- in the inverted potential $-V(\theta_-)$, where θ_- corresponds to position and x to time. Near the first-order I-F transition, $V(\theta_-)$ has local minima at $\theta_-=0$ and $\pi/6$ (mod $2\pi/6$), and hence $-V(\theta_-)$ has maxima at those locations. The minimum-energy profile $\theta_-(x)$ therefore has the form shown in Fig. 8: $\theta_-(x)$ goes from 0 to $\pi/6$ in a short distance $\xi_{1/2}$, it remains close to $\pi/6$ for a much longer distance w, and then it goes from $\pi/6$ to $2\pi/6$ in a distance $\xi_{1/2}$. The total arm width is $\xi=w+2\xi_{1/2}$. The arm therefore contains a sliver of the incipient, metastable F phase with thickness w. As $h_6\to 0+$, this sliver of F thickens. Integration of Eq. (6.6) gives

$$w\approx\sqrt{K_-/2}\int_{\pi/12}^{3\pi/12}d\theta_-\frac{1}{\sqrt{V(\theta_-)-V(0)}}$$
$$\approx\frac{1}{12}\left[\frac{K_-}{h_{12}}\right]^{1/2}\ln\left[\frac{h_{12}}{h_6}\right]. \tag{6.11}$$

This behavior is similar to complete wetting. As $h_6\to 0+$, the F phase "wets" the interior of the arm.

We can look at this system from a more macroscopic point of view. We can think of the profile in Fig. 8 as a pair of "half-arms," each with width $\xi_{1/2}$ and energy $\varepsilon_{1/2}$ per unit length, separated by a region of the F phase with width w. By analogy with Eqs. (6.9) and (6.10), we find

$$\xi_{1/2}=\tfrac{1}{12}\sqrt{K_-/h_{12}}\ , \tag{6.12a}$$

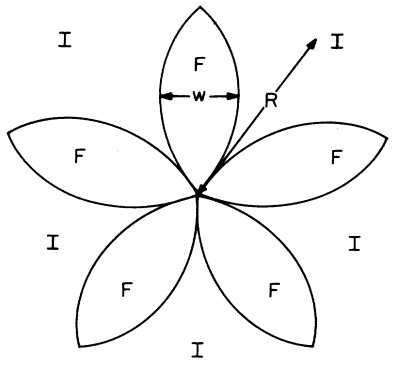

FIG. 9. Form of the star defect in the I phase very close to the first-order I-F transition. When the arms become this thick, the divergence of w is cut off.

$$\varepsilon_{1/2}=\tfrac{2}{3}\sqrt{K_-h_{12}}\ . \tag{6.12b}$$

The two half-arms repel each other with an interaction energy of range $\xi_{1/2}$ and strength $R\,\varepsilon_{1/2}$. There is also an energy penalty of $2h_6Rw$ for the region of the F phase between the half-arms. The energy of a whole arm per unit length is then

$$\varepsilon=2\varepsilon_{1/2}+\varepsilon_{1/2}e^{-w/\xi_{1/2}}+2h_6w\ . \tag{6.13}$$

By minimizing this expression over w, we find that w increases logarithmically as $h_6\to 0+$ exactly as in Eq. (6.11).

So far we have simply minimized the energy of an arm in mean-field theory. At any nonzero temperature, however, the two half-arms can fluctuate. We can think of the half-arms as random walks, each with diffusion constant $(12\varepsilon_{1/2})^{-1}$, which cannot cross. When the half-arms are close to each other, they have less room to fluctuate, and hence have a lower entropy. Several calculations[21] have shown that the interaction between two random walks that cannot cross can be expressed as an effective entropic repulsion. By the argument of Fisher,[21] the entropic repulsion between two half-arms (per unit length, normalized by k_BT) is

$$\varepsilon_{\text{entropic}}=\frac{1}{12\varepsilon_{1/2}w^2}\ . \tag{6.14}$$

This term must be added to the right-hand side of Eq. (6.13) to obtain the free energy of a whole arm per unit length. For $w\gg\xi_{1/2}$, the entropic repulsion is much greater than the exponential repulsion. Minimizing the free energy of the whole arm over w gives the equilibrium arm width

$$w\approx(12\varepsilon_{1/2}h_6)^{-1/3}\ . \tag{6.15}$$

Close to the I-F transition, $h_6\propto(T-T_{IF})$. The equilibrium arm width therefore increases as $(T-T_{IF})^{-1/3}$. This $\frac{1}{3}$ power law has been found in other theoretical studies of wetting in 2D.[22,23] The star defect may provide an opportunity to observe this power law.

We must make two comments about the power-law

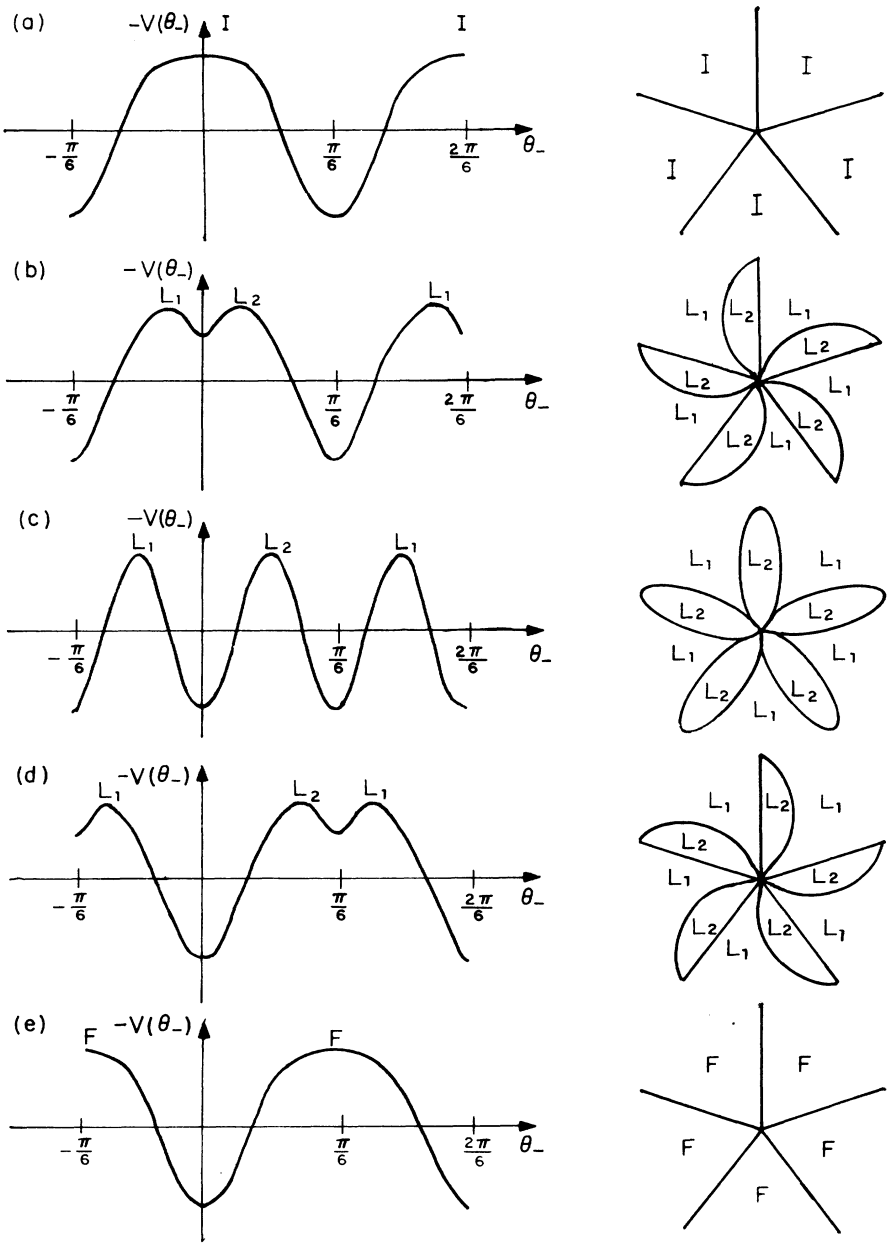

FIG. 10. Sequence of inverted potentials $-V(\theta_-)$, and the corresponding forms of the star defect, in a material with $h_{12}<0$: (a) $h_6=h_6^{IL}$. (b) $0<h_6<h_6^{IL}$. (c) $h_6=0$. (d) $h_6^{LF}<h_6<0$. (e) $h_6=h_6^{LF}$.

divergence of w. First, note that the arm energy ε decreases toward the finite limit $2\varepsilon_{1/2}$ as $h_6\to 0+$. Hence, as we approach the I-F transition the arm length R increases and the defect energy ΔE decreases. However, R remains finite at the transition. For this reason, the star defect cannot be a nucleus for the growth of the F phase until one undercools a finite distance beyond the first-order transition. In contrast with some transitions involving complete wetting, the first-order I-F transition occurs with some (possibly small) hysteresis. Second, note that the thin-arm approximation breaks down when the defect arms thicken into the wide petals shown in Fig. 9. When we are this close to the transition, we can no longer treat each arm as isolated and uniform along its length. The power-law divergence of w is cut off when w grows to the order of $w_{\max}\approx\sqrt{R/\varepsilon_{1/2}}$. In experiments[5] $R\approx 1$ mm. Nevertheless, the $\frac{1}{3}$ power law should apply over a wide range of reduced temperature, as w grows from microscopic lengths to $w_{\max}$, and the defect arms thicken from the form in Fig. 7 to the form in Fig. 9.

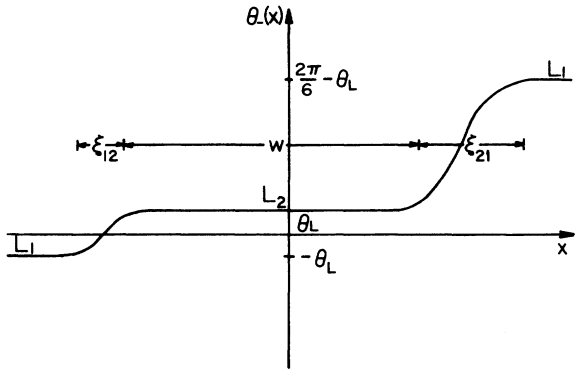

FIG. 11. Profile $\theta_-(x)$ across one arm for $0<h_6<h_6^{\rm IL}$. The difference angle $\theta_-=-\theta_L$ (mod $2\pi/6$) in the L_1 phase and $+\theta_L$ (mod $2\pi/6$) in the L_2 phase. Across the arm, θ_- goes from L_1 to L_2 in a half-arm of width ξ_{12}, and it goes from L_2 to L_1 in a half-arm of width ξ_{21}.

At the present time the star defect has only been observed in thin films of thermotropic liquid crystals, which have $h_{12}>0$. However, this defect might also be observed in materials in which $h_{12}<0$. We therefore consider the behavior of this defect near the *I-L* and *L-F* transitions. To understand what happens to an arm near these transitions, we return to Eq. (6.6) and its analogy in classical mechanics. Consider the motion of a classical particle in the inverted potentials $-V(\theta_-)$ of Fig. 10. As h_6 decreases toward h_6^{IL}, there are no major changes in the arm. At h_6^{IL} the system undergoes an Ising-type transition from I to L. There are really two L phases, L_1 and L_2, which are mirror images of each other, like the spin-up and spin-down phases of an Ising ferromagnet. One of these L phases is selected as the bulk phase by spontaneous symmetry breaking. Suppose that L_1 is the bulk phase. The resulting profile $\theta_-(x)$ is shown in Fig. 11. The system goes from L_1 to L_2 in a half-arm of width ξ_{12} (with line energy ε_{12}), it remains in the L_2 phase for a distance w, and then it goes from L_2 back to L_1 in a half-arm of width ξ_{21} (with line energy ε_{21}). Because L_1 and L_2 have exactly the same energy, there is no penalty for the width w of L_2 inside the arm. Therefore, the thin-arm approximation does not apply, and w can be of the order of $\sqrt{R/\varepsilon_{12}}+\sqrt{R/\varepsilon_{21}}$ for all h_6 between h_6^{IL} and h_6^{LF}.

Note that the half-arm widths and the corresponding energies are unequal, $\xi_{12}\neq\xi_{21}$ and $\varepsilon_{12}\neq\varepsilon_{21}$, unless $h_6=0$. The higher-energy half-arm is shorter, and the lower-energy half-arm is longer. The star defect therefore goes through the sequence of structures shown in Fig. 10. If $0<h_6<h_6^{IL}$, the defect has a chiral, "pinwheel" form even if the underlying material is not chiral. The direction of the pinwheel is determined by the direction of the vorticity and by the spontaneous symmetry breaking that chose L_1 as the bulk phase. At $h_6=0$ the defect is symmetric. If $h_6^{LF}<h_6<0$, the defect is chiral again, but with the opposite chirality. For $h_6<h_6^{\rm LF}$, the system is in the F phase, and the arms are thin again.

ACKNOWLEDGMENTS

We are grateful to S. B. Dierker, R. Lipowsky, R. Pindak, H. S. Seung, E. B. Sirota, and T. J. Sluckin for many helpful discussions. This work was supported by the National Science Foundation through Grant No. DMR 85-14638 and through the Harvard Materials Research Laboratory.

[1]G. S. Smith, E. B. Sirota, C. R. Safinya, and N. A. Clark, Phys. Rev. Lett. **60**, 813 (1988).
[2]D. R. Nelson and B. I. Halperin, Phys. Rev. B **21**, 5312 (1980).
[3]S. B. Dierker and R. Pindak, Phys. Rev. Lett. **59**, 1002 (1987).
[4]J. V. Selinger and D. R. Nelson, Phys. Rev. Lett. **61**, 416 (1988).
[5]S. B. Dierker, R. Pindak, and R. B. Meyer, Phys. Rev. Lett. **56**, 1819 (1986).
[6]D. R. Nelson and L. Peliti, J. Phys. (Paris) **48**, 1085 (1987); **49**, 139 (1988).
[7]F. David, E. Guitter, and L. Peliti, J. Phys. (Paris) **48**, 2059 (1987).
[8]J. V. Selinger, J. Phys. (Paris) **49**, 1387 (1988).
[9]This observation is due to H. S. Seung.
[10]For a review, see T. J. Sluckin and A. Poniewierski, in *Fluid Interfacial Phenomena*, edited by C. A. Croxton (Wiley, New York, 1986), Sec. 5.3.1.
[11]J. B. Kogut, Rev. Mod. Phys. **51**, 659 (1979), Sec. VII D; see also K. G. Wilson and J. B. Kogut, Phys. Rep. C **12**, 75 (1974), Sec. 11; T. Ohta and D. Jasnow, Phys. Rev. B **20**, 139 (1979), Appendix.
[12]K. Y. Szeto and G. Dresselhaus, Phys. Rev. B **32**, 3186 (1985).
[13]D. R. Nelson, in *Phase Transitions and Critical Phenomena*, edited by C. Domb and J. L. Lebowitz (Academic, New York, 1983), Vol. 7, Sec. II-E, and references therein.
[14]J. M. Kosterlitz, J. Phys. C **7**, 1046 (1974).
[15]K. Y. Szeto and G. Dresselhaus, Phys. Rev. B **32**, 3142 (1985).
[16]D. R. Nelson and R. A. Pelcovits, Phys. Rev. B **16**, 2191 (1977).
[17]H. S. Seung and D. R. Nelson, Phys. Rev. A **38**, 1005 (1988).
[18]E. B. Sirota, J. Phys. (Paris) **49**, 1443 (1988).
[19]In evaluating the integral in Eq. (6.1), we make one approximation: instead of excluding only the defect cores, we exclude the entire annulus $R-a<r<R+a$ from the integral. This approximation should only have a very small effect on the result.
[20]S. B. Dierker (private communication).
[21]M. E. Fisher, J. Stat. Phys. **34**, 667 (1984), Sec. 9–10 and references therein.
[22]D. B. Abraham and E. R. Smith, Phys. Rev. B **26**, 1480 (1982).
[23]R. Lipowsky, D. M. Kroll, and R. K. P. Zia, Phys. Rev. B **27**, 4499 (1983).